Received: 28 February 2017 | Revised: 9 April 2017 | Accepted: 22 April 2017

DOI: 10.1002/aoc.3893

FULL PAPER

WILEY Applied Organometallic Chemistry

Ring-opening polymerization of lactide, ε-caprolactone and their copolymerization catalyzed by β-diketiminate zinc complexes

Maryam Keram | Haiyan Ma

Shanghai Key Laboratory of Functional Materials Chemistry and Laboratory of Organometallic Chemistry, School of Chemistry and Molecular Engineering, East China University of Science and Technology, 130 Meilong Road, Shanghai 200237, China

Correspondence
Haiyan Ma, Shanghai Key Laboratory of Functional Materials Chemistry and Laboratory of Organometallic Chemistry, School of Chemistry and Molecular Engineering, East China University of Science and Technology, 130 Meilong Road, Shanghai 200237, China.
Email: haiyanma@ecust.edu.cn

Funding information
National Natural Science Foundation of China, Grant/Award Number: 21074032 and 21474028; Fundamental Research Funds for the Central Universities, Grant/Award Number: WD1113011

A series of zinc silylamido complexes bearing non-symmetric β-diketiminate ligands were synthesized and structurally characterized. Ring-opening polymerization (ROP) of *rac*-lactide catalyzed by these zinc complexes afforded heterotactic polylactides at room temperature (P_r = 0.79 ~ 0.83 in THF). The steric and electronic characteristics of the ancillary ligands showed significant influence on the polymerization performance of the corresponding zinc complexes. All these zinc complexes also showed moderate activities toward the polymerization of ε-caprolactone at ambient temperature in toluene, producing polycaprolactones (PCLs) with high molecular weights and moderate polydispersities. PCL-*b*-PLLA copolymers could be obtained via three different copolymerization strategies (one-pot polymerization, and sequential addition of the two monomers in either order) by adopting complex **6** as the initiator through the adjustment of reaction temperatures. The diblock nature of the copolymers was confirmed by ^{13}C NMR spectroscopy and DSC analysis.

KEYWORDS
copolymerization, lactide, ring-opening polymerization, zinc complex, ε-caprolactone

1 | INTRODUCTION

Aliphatic polyesters, such as polylactide, poly(ε-caprolactone) and their copolymers, have been taken great attention due to their biodegradability, biocompatibility and therefore their wide potentials utilized as drug-delivery, surgical suture and artificial tissue materials.[1a] Up to date, a variety of well-defined metal complexes capable of initiating the ROP of the related cyclic esters have been reported.[1b-k] Among them, complexes of groups 1[2–5] and 2[6] metals as well as zinc[7] have attracted great interests due to the low toxicity of the elements and the good control of the complexes over the polymerization processes. As an environmental friendly metal, zinc has relatively less ionic nature when compared to groups 1 and 2 metals, and the filled *d* orbitals when it is in the normal oxidation state of Zn(II) also allow lower coordination numbers; both of these features are especially beneficial to the construction of well-defined zinc complexes. Being widely adopted as ligands for various metals, the class of β-diketimine (BDI) ligand frameworks also assumes a special position in zinc initiators adopted for *rac*-lactide (*rac*-LA) polymerization due to its ease in accessibility and variability.[7k-p, 8-10] Typically, highly heterotactic PLAs (P_r = 0.94) were obtained by a series of symmetrically substituted β-diketiminate zinc complexes at 0°C within 20 h reaction periods.[8] When one of the *N*-(2,6-diisopropyl)phenyl groups was replaced by *N*-*ortho*-methoxyphenyl, the resultant unsymmetrical β-diketimine proligand led to zinc complexes showing higher activities but significant lower heteroselectivities when compared to the symmetrical counterparts (slightly heteroselective *vs.* P_r = 0.90).[9] Schaper and co-workers[10] further introduced chiral *N*-(*S*)-phenylethyl to construct C_2-symmetric zinc diketiminate

complexes which however still afforded heterotactic PLAs ($P_r = 0.84 \sim 0.88$). Clearly, the ancillary ligand frameworks played an important role in the stereochemistry of resultant polymers; however, despite the numerous efforts that have been devoted to this chemistry, the relationship between the structure and stereoselectivity of β-diketiminate zinc catalysts toward *rac*-lactide polymerization is still ambiguous.

In order to achieve more stereoselective polymerization of *rac*-lactide, our group previously reported a series of non-symmetric β-diketiminate aluminum complexes for the ROP of cyclic esters.[11] Nevertheless, those aluminum complexes are only active for the polymerization of ε-caprolactone at 80°C, but inactive for *rac*-lactide polymerization. Meanwhile, the related zinc complexes were not studied extensively. As a part of our research, we are interested in obtaining some non-symmetric BDI zinc complexes and further exploring their catalytic activities and selectivities toward the ROP of cyclic esters.

On the other hand, various metal complexes based on aluminum,[12] zinc,[13] titanium,[14] rare earth metals[15,16] and stannous[17,18] are also known as efficient initiators for the copolymerization of ε-caprolactone and lactide. For instance, homosalen aluminum complexes reported by Nomura and co-workers[19] could afford copolymers with high random sequences. Lately, our group reported[20] some dinuclear salan aluminum complexes, which produced blocky, gradient, tapered and random copolymers with the variation of temperature, monomer-initiator ratio and the amount of excess alcohol. Recently, Lamberti and co-workers[21] reported that salalen aluminum complexes could initiate the random copolymerization of ε-CL/LA in a controlled manner at 80°C in toluene. Titanium complexes bearing pyridonate ligands reported by Schafer and co-workers could form block (at 100°C) and random copolymers (at 130°C).[14] Tridentate Schiff base zinc complexes derived from natural amino acid phenylalanine afforded random ε-CL/*L*-LA copolymers in melt.[13a] More recently, trisalkyl- or alkyl-aryloxide zinc complexes were reported to form random copolymers at 90°C.[22] It is worth noting that, in most cases, diblock copolymers could only be produced via the sequential addition of lactide after the full conversion of ε-CL; block or random copolymers were hardly formed when reversed feeding strategy or one pot addition was adopted, which normally is suggested to be due to the energy barrier of the last ring-opened LA monomer coordinating to the metal center. Therefore, most of the reported copolymerization procedures require higher polymerization temperature; to the best of our knowledge, very rare examples of ε-CL/*L*-LA copolymerization succeed under mild reaction conditions. Moreover, to date, there are no reports on the copolymerization behavior of lactide and ε-CL initiated by β-diketimine ligated zinc complexes.

Herein, we reported the synthesis of a series of non-symmetric β-diketiminate zinc complexes and investigated their catalytic performance toward the ROP of *rac*-LA and ε-CL in different solvents at ambient temperature. The copolymerization of *L*-LA and ε-CL was also studied by adopting different feeding strategies.

2 | EXPERIMENTAL

2.1 | General considerations

All manipulations were carried on under a dry argon atmosphere using standard Schlenk-line or glove box techniques. Toluene and *n*-hexane were refluxed over sodium benzophenone ketyl prior to use. Benzene-d_6, chloroform-*d* and other reagents were properly dried and stored in the glove-box. $Zn[N(SiMe_3)_2]_2$ was synthesized according to the literature procedure.[23] *rac*-Lactide, *L*-lactide (Aldrich) were sublimed 3 times under vacuum at 80°C and then recrystallized with toluene. ε-Caprolactone (from Aldrich) was dried over CaH_2 for 24 h at 50°C and then distilled under reduced pressure. 2-Propanol was dried over calcium hydride prior to distillation. All other chemicals were commercially available and used after appropriate purification. 4-((2,6-Diisopropylphenyl)amino)pent-3-en-2-one, 2-(2,6-diisopropylphenyl)amino-4-(4-isopropylphenyl)imino-2-pentene (**L^4H**), 2-(2,6-diisopropylphenyl)amino-4-(4-chlorophenyl)imino-2-pentene (**L^5H**) and 2-(2,6-diisopropylphenyl)amino-4-(3-fluorophenyl)imino-2-pentene (**L^6H**) were synthesized according to the literature procedures.[11] Glassware and vials used in the polymerization were dried in an oven at 120°C overnight and exposed to vacuum-argon cycle three times.

NMR spectra (^1H NMR, 400 MHz; ^{13}C NMR, 100 MHz) were recorded on a Bruker AVANCE-400 spectrometer at 25°C, referenced internally using the residual solvent resonances and reported relative to tetramethylsilane. Elemental analyses were carried on an EA-1106 instrument. Gel permeation chromatography (GPC) analyses were carried on a Waters 1515 Breeze instrument in THF at 35°C, at a flow rate of 1 ml/min. Calibration standards were commercially available narrowly distributed linear polystyrene samples that cover a broad range of molar masses ($6 \times 10^3 < M < 6 \times 10^6$ g/mol). Differential scanning calorimetric (DSC) curves were taken on a Perkin-Elmer Pyris 1 instrument. All samples were cooled to −40°C and heated to 200°C for the first scan. After being kept for 1 min, they were again cooled to −40°C and heated to 200°C then cooled to −40°C for the second cycle. The heating rate was 10°C min^{-1}.

2.2 | Synthesis of β-diketimine proligands and zinc complexes

2.2.1 | 2-(2,6-Diisopropylphenyl)amino-4-(2-methylphenyl)imino-2-pentene (L^1H)

To a stirred solution of *o*-toluidine (2.67 g, 24.9 mmol) in 75 ml of toluene was added *para*-toluenesulfonic acid monohydrate (4.75 g, 25.0 mmol), and the mixture was continuously stirred for 3 h at room temperature, then 4-((2,6-diisopropylphenyl)amino)pent-3-en-2-one[11] (6.50 g, 25.0 mmol) was added to the mixture solution. A Dean–Stark apparatus was attached and the mixture was heated to reflux for 24 h. The reaction mixture was cooled to room temperature and dried under reduced pressure to give a yellow solid. The obtained solid was treated with diethyl ether (25 ml), water (25 ml) and sodium carbonate (2.50 g, 25.0 mmol), and kept stirring. After complete dissolution, the aqueous phase was separated and extracted with diethyl ether. The combined organic phases were dried over $MgSO_4$ and rotary evaporated to dryness under reduced pressure to afford a yellow solid. Recrystallization of this crude material with methanol afforded **L^1H** as light yellow prismatic crystals (4.00 g, 46%). Mp: 93–95 °C. ^{1}H NMR (400 MHz, 298 K, $CDCl_3$): δ 12.41 (br, 1H, N*H*), 7.17–7.10 (m, 5H, Ar*H*), 6.99 (td, ^3J = 7.4 Hz, ^2J = 1.0 Hz, 1H, Ar*H*), 6.91 (d, ^3J = 7.8 Hz, 1H, Ar*H*), 4.89 (s, 1H, γ-C*H*), 3.06 (sept, ^3J = 6.8 Hz, 2H, C*H* (CH_3)$_2$), 2.19 (s, 3H, CH_3), 1.92 (s, 3H, CH_3), 1.70 (s, 3H, CH_3), 1.21 (d, ^3J = 6.8 Hz, 6H, CH(CH_3)$_2$), 1.11 (d, ^3J = 6.8 Hz, 6H, CH(CH_3)$_2$). ^{13}C NMR (100 MHz, 298 K, $CDCl_3$): δ 161.7 (N*C*Me), 159.5 (N*C*Me), 144.8, 142.3, 141.2, 131.1, 130.5, 126.4, 125.2, 123.8, 123.4, 123.2, (all Ar-C), 95.1 (γ-*C*H), 28.5 (*C*H(CH$_3$)$_2$), 24.5 (CH(*C*H$_3$)$_2$), 23.1 (CH(*C*H$_3$)$_2$), 21.0 (NC-*C*H$_3$), 20.9 (NC-*C*H$_3$), 18.4 (Ar-*C*H$_3$). IR (KBr, cm^{-1}): 3032w, 2960 m, 2923 m, 2866 m, 1622s, 1547s, 1478 m, 1459 m, 1378 m, 1258s, 1176 m, 1096s, 1021s, 860 m, 792 s. Anal. Calcd. for $C_{24}H_{32}N_2$: C 82.71, H 9.25, N 8.04; found: C 82.33, H 9.03, N 7.93%.

2.2.2 | 2-(2,6-Diisopropylphenyl)amino-4-(2-isopropylphenyl)imino-2-pentene (L^2H)

Proligand **L^2H** was synthesized by the same procedure as **L^1H**. 2-Isopropylaniline (3.44 g, 25.7 mmol), 4-((2,6-diisopropylphenyl)amino)pent-3-en-2-one (6.50 g, 25.0 mmol) and *para*-toluene sulfonic acid monohydrate (4.75 g, 25.0 mmol) were used to give **L^2H** as light yellow prismatic crystals (6.6 g, 72%). Mp: 80–82°C. ^{1}H NMR (400 MHz, 298 K, $CDCl_3$): δ 12.39 (br s, 1H, N*H*), 7.28–7.26 (m, 2H, Ar*H*), 7.25 (br s, 2H, Ar*H*, overlapped with $CDCl_3$), 7.14–7.07 (m, 2H, Ar*H*), 6.89 (td, ^3J = 7.4 Hz, ^4J = 1.3 Hz, 1H, Ar*H*), 4.90 (s, 1H, γ-C*H*), 3.20 (sept, ^3J = 6.8 Hz, 1H, C*H*(CH$_3$)$_2$), 3.09 (sept, ^3J = 6.8 Hz, 2H, C*H*(CH$_3$)$_2$), 1.92 (s, 3H, CH_3), 1.72 (s, 3H, CH_3), 1.23 (d, ^3J = 6.8 Hz, 6H, CH(CH$_3$)$_2$), 1.17 (d, ^3J = 6.8 Hz, 3H, CH(CH$_3$)$_2$), 1.16 (d, ^3J = 6.8 Hz, 3H, CH(CH$_3$)$_2$), 1.13 (d, ^3J = 6.8 Hz, 12H, CH(CH$_3$)$_2$). ^{13}C NMR (100 MHz, 298 K, $CDCl_3$): δ 161.3 (N*C*Me), 160.2 (N*C*Me), 143.6, 142.6, 141.8, 140.9, 126.0, 125.7, 125.3, 124.4, 124.0, 123.2, (all Ar-C), 94.9 (γ-*C*H), 28.4 (*C*H(CH$_3$)$_2$), 28.2 (*C*H(CH$_3$)$_2$), 24.4 (CH(*C*H$_3$)$_2$), 23.4 (CH(*C*H$_3$)$_2$), 23.1 (CH(*C*H$_3$)$_2$), 21.0 (NC-*C*H$_3$), 20.9 (NC-*C*H$_3$). IR (KBr, cm^{-1}): 3031w, 2959 m, 2922 m, 2864 m, 1626 m, 1555 m, 1503 m, 1438 m, 1380 m, 1277 m, 1216 m, 1099 m, 1027 m, 805 m, 750 s. Anal. Calcd. for $C_{26}H_{36}N_2$: C 82.94, H 9.64, N 7.44; found: C 82.91, H 9.70, N 7.45%.

2.2.3 | 2-(2,6-Diisopropylphenyl)amino-4-(2-chlorophenyl)imino-2-pentene (L^3H)

Proligand **L^3H** was synthesized by the same procedure as **L^1H**. 2-Chloroaniline (3.20 g, 25.0 mmol), 4-((2,6-diisopropylphenyl)amino)pent-3-en-2-one (6.50 g, 25.0 mmol) and *para*-toluene sulfonic acid monohydrate (4.75 g, 25.0 mmol) were used to give **L^3H** as light yellow prismatic crystals (6.05 g, 66%). Mp: 77–79°C. ^{1}H NMR (400 MHz, 298 K, $CDCl_3$): δ 12.28 (br, 1H, N*H*), 7.34 (dd, ^3J = 7.8 Hz, ^4J = 1.1 Hz, 1H, Ar*H*), 7.22–7.16 (m, 2H, Ar*H*), 7.15 (br s, 1H, Ar*H*), 7.12 (m, 1H, Ar*H*), 6.96–6.91 (m, 2H, Ar*H*), 4.93 (s, 1H, γ-C*H*), 3.14 (sept, J = 6.8 Hz, 2H, C*H*(CH$_3$)$_2$), 1.92 (s, 3H, CH_3), 1.71 (s, 3H, CH_3), 1.23 (d, ^3J = 6.8 Hz, 6H, CH(CH_3)$_2$), 1.13 (d, ^3J = 6.8 Hz, 6H, CH(CH_3)$_2$). ^{13}C NMR (100 MHz, 298 K, $CDCl_3$): δ 161.1 (N*C*Me), 160.4 (N*C*Me), 148.5, 142.9, 139.9, 134.5, 129.9, 125.9, 123.3, 122.7, 122.2, 120.5, (all Ar-C), 96.1 (γ-*C*H), 28.6 (*C*H(CH$_3$)$_2$), 24.6 (CH(*C*H$_3$)$_2$), 22.8 (CH(*C*H$_3$)$_2$), 21.2 (NC-*C*H$_3$), 20.8 (NC-*C*H$_3$). IR (KBr, cm^{-1}): 3033w, 2961 m, 2923 m, 2867 m, 1622s, 1547s, 1486 m, 1462 m, 1378 m, 1259s, 1181 m, 1096s, 1026 m, 928 m, 753 s. Anal. Calcd. for $C_{23}H_{29}ClN_2$: C 74.88, H 7.92, N 7.59; found: C 74.89, H 7.96, N 7.57%.

2.2.4 | 2-(2,6-Diisopropylphenyl)amino-4-(3-chlorophenyl)imino-2-pentene (L^7H)

Proligand **L^7H** was synthesized by the same procedure as **L^1H**. 3-Chloroaniline (3.00 g, 23.5 mmol), 4-((2,6-diisopropylphenyl)amino)pent-3-en-2-one (6.50 g, 25.0 mmol) and *para*-toluene sulfonic acid monohydrate (4.75 g, 25.0 mmol) were used to give **L^7H** as light yellow prismatic crystals (6.56 g, 71%). Mp: 93–95°C. ^{1}H NMR (400 MHz, 298 K, $CDCl_3$): δ 12.28 (br, 1H, N*H*), 7.18–7.11 (m, 4H, Ar*H*), 6.94 (d, ^3J = 8.0 Hz, 1H, Ar*H*), 6.88 (t, ^4J = 2.0 Hz, 1H, Ar*H*), 6.75 (d, ^3J = 8.0 Hz, 1H, Ar*H*), 4.88 (s, 1H, γ-C*H*), 3.02 (sept, ^3J = 6.8 Hz, 2H, C*H*(CH$_3$)$_2$), 2.02 (s, 3H, CH_3), 1.68 (s, 3H, CH_3), 1.22 (d, ^3J = 6.8 Hz, 6H,

CH(CH_3)$_2$), 1.13 (d, ^3J = 6.8 Hz, 6H, CH (CH_3)$_2$). ^{13}C NMR (100 MHz, 298 K, $CDCl_3$): δ 161.1 (N*C*Me), 160.4 (N*C*Me), 148.5, 142.9, 139.9, 134.5, 129.9, 125.9, 123.7, 123.3, 122.2, 120.5 (all Ar-C), 96.1 (γ-*C*H), 28.6 (*C*H(CH$_3$)$_2$), 22.8 (CH(*C*H$_3$)$_2$), 21.2 (NC-*C*H$_3$), 20.8 (NC-*C*H$_3$). IR (KBr, cm^{-1}): 3035w, 2959 m, 2924 m, 2866 m, 1622s, 1545s, 1461 m, 1438 m, 1378 m, 1258s, 1176 m, 1094 m, 1020s, 871 m, 759 s. Anal. Calcd. for $C_{23}H_{29}ClN_2$: C 74.88, H 7.92, N 7.59; found: C 74.89, H 7.96, N 7.57%.

2.2.5 | 2-(2,6-Diisopropylphenyl)amino-4-(2-methyl-5-chloro)imino-2-pentene (L^{8}H)

Proligand **L^{8}H** was synthesized by the same procedure as **L^{1}H**. 5-Chloro-2-methylaniline (3.50 g, 24.7 mmol), 4-((2,6-diisopropylphenyl)amino)pent-3-en-2-one (6.50 g, 25.0 mmol) and *para*-toluene sulfonic acid monohydrate (4.75 g, 25.0 mmol) were used to give **L^{8}H** as light yellow prismatic crystals (8.00 g, 83%). Mp: 88–90°C. ^{1}H NMR (400 MHz, 298 K, $CDCl_3$): δ 12.28 (br, 1H, N*H*), 7.21–7.12 (m, 4H, Ar*H*), 7.05 (d, ^3J = 8.0 Hz, 1H, Ar*H*), 6.90 (dd, ^3J = 8.0 Hz, ^4J = 2.0 Hz, 1H, Ar*H*), 6.83 (d, ^2J = 2.0 Hz, 1H, Ar*H*), 4.90 (s, 1H, γ-C*H*), 3.08 (sept, ^3J = 6.8 Hz, 2H, C*H*(CH$_3$)$_2$), 2.10 (s, 3H, CH_3), 1.90 (s, 3H, CH_3), 1.69 (s, 3H, CH_3), 1.22 (d, ^3J = 6.8 Hz, 6H, CH(CH_3)$_2$), 1.11 (d, ^3J = 6.8 Hz, 6H, CH(CH_3)$_2$). ^{13}C NMR (100 MHz, 298 K, $CDCl_3$): δ 162.3 (N*C*Me), 159.8 (N*C*Me), 148.4, 144.1, 138.5, 131.4, 131.3, 128.5, 126.4, 123.3, 122.9, 121.9 (all Ar-C), 95.1 (γ-*C*H), 28.6 (*C*H(CH$_3$)$_2$), 24.7 (CH(*C*H$_3$)$_2$), 22.9 (CH(*C*H$_3$)$_2$), 21.3 (NC-*C*H$_3$), 20.5 (NC-*C*H$_3$), 17.9 (Ar-*C*H$_3$). IR (KBr, cm^{-1}): 3034w, 2961 m, 2925 m, 2868 m, 1612s, 1552s, 1494 m, 1444 m, 1359 m, 1274s, 1176 m, 1082 m, 1019 m, 870 m, 794 s. Anal. Calcd. for $C_{24}H_{31}ClN_2$: C 75.27, H 8.16, N 7.31; found: C 75.07, H 8.21, N 7.25%.

2.2.6 | [L^{1}ZnN(SiMe$_3$)$_2$] (1)

A solution of **L^{1}H** (0.52 g, 1.5 mmol) in toluene (15 ml) was added into zinc bis(trimethylsilyl)amide (0.58 g, 1.5 mmol) in toluene (5 ml) at room temperature. After being stirred for 12 h at 80°C, the resultant clear yellow-green solution was dried under vacuum to give light yellow solids. After recrystallization with hexane (5 ml) at −40°C, light yellow crystals were obtained (250 mg, 47%). Mp: 107–109°C. ^{1}H NMR (400 MHz, 298 K, C_6D_6): δ 7.14–7.11 (m, 2H, Ar*H*), 7.11–7.08 (m, 2H, Ar*H*), 7.06–7.04 (m, 2H, Ar*H*), 6.97 (td, ^3J = 7.3 Hz, ^2J = 1.5 Hz, 1H, Ar*H*), 4.83 (s, 1H, γ-C*H*), 3.41 (sept, ^3J = 6.8 Hz, 1H, C*H*(CH$_3$)$_2$), 3.20 (sept, ^3J = 6.8 Hz, 1H, C*H*(CH$_3$)$_2$), 2.16 (s, 3H, CH_3), 1.65 (s, 3H, CH_3), 1.59 (s, 3H, CH_3), 1.43 (d, ^3J = 6.8 Hz, 3H, CH(CH_3)$_2$), 1.32 (d, ^3J = 6.8 Hz, 3H, CH(CH_3)$_2$), 1.16 (d, ^3J = 6.8 Hz, 3H, CH(CH_3)$_2$), 1.12 (d, ^3J = 6.8 Hz, 3H, CH(CH_3)$_2$), 0.17 (s, 9H, N(Si(CH_3)$_3$)$_2$), −0.13 (s, 9H, N(Si(CH_3)$_3$)$_2$). ^{13}C NMR (100 MHz, 298 K, $CDCl_3$): δ 170.0 (N*C*Me), 168.8 (N*C*Me), 148.2, 144.7, 142.8, 142.5, 132.0, 131.4, 127.3, 126.8, 126.7, 126.0, 124.7, 124.6 (all Ar-C), 96.1 (γ-*C*H), 28.9 (*C*H(CH$_3$)$_2$), 28.8 (*C*H(CH$_3$)$_2$), 25.5 (CH(*C*H$_3$)$_2$), 25.0 (CH(*C*H$_3$)$_2$), 24.9 (CH(*C*H$_3$)$_2$), 24.8 (CH(*C*H$_3$)$_2$), 24.6 (NC-*C*H$_3$), 23.8 (NC-*C*H$_3$), 18.6 (Ar-*C*H$_3$), 5.9 (Si(*C*H$_3$)$_3$), 5.5 (Si(*C*H$_3$)$_3$). Anal. Calcd. for $C_{30}H_{49}N_3Si_2Zn$: C 62.85, H 8.62, N 7.33; found: C 62.43, H 8.76, N 7.26%.

2.2.7 | [L^{2}ZnN(SiMe$_3$)$_2$] (2)

The same procedure as that of complex **1** was adopted. **L^{2}H** (0.58 g, 1.5 mmol) and zinc bis(trimethylsilyl)amide (0.58 g, 1.5 mmol) were used to afford light yellow crystals (192 mg, 32%). Mp: 126–127°C. ^{1}H NMR (400 MHz, 298 K, $CDCl_3$): δ 7.20 (dd, ^3J = 7.2 Hz, ^4J = 2.0 Hz, 1H, Ar*H*), 7.13–7.03 (m, 4H, Ar*H*), 6.90 (dd, ^3J = 7.2 Hz, ^4J = 2.0 Hz, 1H, Ar*H*), 4.82 (s, 1H, γ-C*H*), 3.37 (sept, ^3J = 6.8 Hz, 1H, −C*H*(CH$_3$)$_2$), 3.29 (sept, ^3J = 6.8 Hz, 1H, −C*H*(CH$_3$)$_2$), 3.15 (sept, ^3J = 6.8 Hz, 1H, −C*H*(CH$_3$)$_2$), 1.66 (s, 3H, CH_3), 1.65 (s, 3H, CH_3), 1.47 (d, ^3J = 6.8 Hz, 3H, −CH(CH_3)$_2$), 1.33 (d, ^3J = 6.8 Hz, 3H, −CH(CH_3)$_2$), 1.31 (d, ^3J = 6.8 Hz, 3H, −CH(CH_3)$_2$), 1.17 (d, ^3J = 6.8 Hz, 3H, −CH(CH_3)$_2$), 1.12 (d, ^3J = 6.8 Hz, 3H, −CH(CH_3)$_2$), 1.06 (d, ^3J = 6.8 Hz, 3H, −CH(CH_3)$_2$), 0.15 (s, 9H, N(Si(CH_3)$_3$)$_2$), −0.14 (s, 9H, N(Si(CH_3)$_3$)$_2$). ^{13}C NMR (100 MHz, 298 K, $CDCl_3$): δ 169.9 (N*C*Me), 168.9 (N*C*Me), 147.1, 144.7, 142.8, 142.4, 142.0, 127.4, 126.8, 126.7, 126.6, 126.4, 124.8, 124.6 (all Ar-C), 96.3 (γ-*C*H), 29.4 (*C*H(CH$_3$)$_2$), 29.1 (*C*H(CH$_3$)$_2$), 28.9 (*C*H(CH$_3$)$_2$), 25.5 (CH(*C*H$_3$)$_2$), 25.1 (CH(*C*H$_3$)$_2$), 24.7 (CH(*C*H$_3$)$_2$), 24.57 (CH(*C*H$_3$)$_2$), 24.54 (CH(*C*H$_3$)$_2$), 24.5 (CH(*C*H$_3$)$_2$), 24.4 (NC-*C*H$_3$), 23.3 (NC-*C*H$_3$), 5.6 (Si(*C*H$_3$)$_3$). Anal. Calcd. For: $C_{32}H_{53}N_3Si_2Zn$: C 63.91, H 8.88, N 6.99; Found: C 63.84, H 8.89, N 6.85%.

2.2.8 | [L^{3}ZnN(SiMe$_3$)$_2$] (3)

The same procedure as that of complex **1** was adopted. **L^{3}H** (0.55 g, 1.5 mmol) and zinc bis(trimethylsilyl)amide (0.58 g, 1.5 mmol) were used to afford light yellow crystals (367 mg, 41%). Mp: 125–127°C. ^{1}H NMR (400 MHz, 298 K, $CDCl_3$): δ 7.24 (dd, ^3J = 8.0 Hz, ^4J = 1.3 Hz, 1H, Ar*H*), 7.13 (brs, 3H), 7.04 (dd, ^3J = 8.0 Hz, ^4J = 1.5 Hz, 1H, Ar*H*), 6.94 (td, ^3J = 8.0 Hz, ^4J = 1.3 Hz, 1H, Ar*H*), 6.70 (td, ^3J = 8.0 Hz, ^4J = 1.5 Hz, 1H, Ar*H*), 4.87 (s, 1H, γ-C*H*), 3.29 (sept, ^3J = 6.8 Hz, 2H, −C*H*(CH$_3$)$_2$), 1.65 (s, 3H, CH_3), 1.39 (d, ^3J = 6.8 Hz, 6H, −CH(CH_3)$_2$), 1.13 (d, ^3J = 6.8 Hz, 6H, −CH(CH_3)$_2$), 0.03 (s, 18H, N(Si(CH_3)$_3$)$_2$). ^{13}C NMR (100 MHz, 298 K, $CDCl_3$): δ 170.8 (N*C*Me), 168.1 (N*C*Me), 146.6, 144.4, 142.7, 130.5, 130.3, 126.9, 126.7, 124.7 (all Ar-C), 96.6 (γ-*C*H), 28.8

($CH(CH_3)_2$), 25.2 ($CH(CH_3)_2$), 24.9 ($CH(CH_3)_2$), 24.7 (NC-CH_3), 23.8 (NC-CH_3), 5.7 ($Si(CH_3)_3$). Anal. Calcd. for $C_{29}H_{46}ClN_3Si_2Zn$: C 58.67, H 7.81, N 7.88; Found: C 58.83, H 7.84, N 7.22%.

2.2.9 | [L^4ZnN($SiMe_3$)$_2$] (4)

The same procedure as that of complex **1** was adopted. L^4H (0.548 g, 1.5 mmol) and zinc bis(trimethylsilyl)amide (0.58 g, 1.5 mmol) were used to afford light yellow crystals (350 mg, 40%). Mp:112–114°C. ^{1}H NMR (400 MHz, 298 K, $CDCl_3$): δ 7.14 (br, 3H, Ar*H*, overlapped with C_6D_6), 7.07 (d, ^3J = 8.3 Hz, 2H, Ar*H*), 6.96 (d, 2H, ^3J = 8.3 Hz, *o*- Ar*H*), 4.86 (s, 1H, γ-C*H*), 3.27 (sept, ^3J = 6.8 Hz, 2H, C*H*(CH_3)$_2$), 2.72 (sept, ^3J = 6.8 Hz, 1H, C*H*(CH_3)$_2$), 1.77 (s, 3H, CH_3), 1.65 (s, 3H, CH_3), 1.37 (d, ^3J = 6.8 Hz, 6H, CH(CH_3)$_2$), 1.16 (d, ^3J = 6.8 Hz, 6H, CH(CH_3)$_2$), 1.12 (d, ^3J = 6.8 Hz, 6H, CH(CH_3)$_2$), 0.00 (s, 18H, N(Si(CH_3)$_3$)$_2$). ^{13}C NMR (100 MHz, 298 K, $CDCl_3$): δ 171.9 (N*C*Me), 168.4 (N*C*Me), 150.9, 143.7, 142.4, 135.4, 130.6, 126.7, 126.0, 125.0, 124.7, 123.9 (all Ar-C), 97.1 (γ-*C*H), 29.0 (*C*H(CH_3)$_2$), 25.1 ($CH(CH_3)_2$), 24.7 ($CH(CH_3)_2$), 24.4 (NC-CH_3), 23.7 (NC-CH_3), 5.2 ($Si(CH_3)_3$). Anal. Calcd. for $C_{32}H_{53}N_3Si_2Zn{\cdot}0.30$ (C_6H_{14}): C 64.75, H 9.10, N 6.71; found: C 65.23, H 8.68, N 6.94%.

2.2.10 | [L^5ZnN($SiMe_3$)$_2$] (5)

The same procedure as that of complex **1** was adopted. L^5H (0.55 g, 1.5 mmol) and zinc bis(trimethylsilyl)amide (0.58 g, 1.5 mmol) were used to afford light yellow crystals (300 mg, 36%). Mp: 180–182°C, ^{1}H NMR (400 MHz, 298 K, $CDCl_3$): δ 7.19 (br s, 2H, Ar-*H*), 7.16–7.13 (m, 3H, Ar-*H*), 6.75 (d, ^3J = 8.8 Hz, 2H, Ar*H*), 4.85 (s, 1H, γ-C*H*), 3.22 (sept, ^3J = 6.8 Hz, 2H, C*H*(CH_3)$_2$), 1.66 (s, 3H, CH_3), 1.65 (s, 3H, CH_3), 1.38 (d, ^3J = 6.8 Hz, 6H, CH(CH_3)$_2$), 1.15 (d, ^3J = 6.8 Hz, 6H, CH(CH_3)$_2$), 0.03 (s, 18H, N(Si(CH_3)$_3$)$_2$). ^{13}C NMR (100 MHz, 298 K, $CDCl_3$): δ 170.5 (N*C*Me), 168.1 (N*C*Me), 147.7, 144.4, 142.5, 131.1, 129.5, 127.7, 127.0, 124.7 (all Ar-C), 96.9 (γ-*C*H), 28.8 (*C*H(CH_3)$_2$), 25.2 ($CH(CH_3)_2$), 24.8 ($CH(CH_3)_2$), 24.7 (NC-CH_3), 24.0 (NC-CH_3), 5.5 ($Si(CH_3)_3$). Anal. Calcd. for $C_{29}H_{46}ClN_3Si_2Zn$: C 58.67, H 7.81, N 7.08; found: C 58.68, H 7.74, N 6.94%.

2.2.11 | [L^6ZnN($SiMe_3$)$_2$] (6)

The same procedure as that of complex **1** was adopted. L^6H (0.53 g, 1.5 mmol) and zinc bis(trimethylsilyl)amide (0.58 g, 1.5 mmol) were used to afford light yellow crystals (380 mg, 44%). Mp: 134–135°C. ^{1}H NMR (400 MHz, 298 K, $CDCl_3$): δ 7.13–7.08 (m, 3H, Ar*H*), 6.93–6.87 (m, 1H, Ar*H*), 6.80–6.79 (m, 1H, Ar*H*), 6.69–6.64 (m, 2H, Ar*H*), 4.79 (s, 1H, γ-C*H*), 3.18 (sept, ^3J = 6.8 Hz, 2H, C*H*(CH_3)$_2$), 1.63 (s, 3H, CH_3), 1.61 (s, 3H, CH_3), 1.33 (d, ^3J = 6.8 Hz, 6H, CH(CH_3)$_2$), 1.10 (d, ^3J = 6.8 Hz, 6H, CH(CH_3)$_2$), − 0.01 (s, 18H, N(Si(CH_3)$_3$)$_2$). ^{13}C NMR (100 MHz, 298 K, $CDCl_3$): δ 170.1 (N*C*Me), 167.5 (N*C*Me), 163.4 (d, $^1J_{FC}$ = 246.9 Hz, Ar-*C*), 150.5 (d, $^3J_{FC}$ = 9.0 Hz, Ar-*C*), 144.4, 142.5, 130.0 (d, $^3J_{FC}$ = 9.0 Hz, Ar-*C*), 127.0, 124.7, 122.2 ($^4J_{FC}$ = 2.8 Hz, Ar-*C*), 112.3 (d, $^2J_{FC}$ = 21.1 Hz, Ar-*C*), 111.7 (d, $^2J_{FC}$ = 21.1 Hz, Ar-*C*) (all Ar-C), 96.9 (γ-*C*H), 28.8 (*C*H(CH_3)$_2$), 25.2 ($CH(CH_3)_2$), 24.8 ($CH(CH_3)_2$), 24.7 (NC-CH_3), 23.9 (NC-CH_3), 5.5 ($Si(CH_3)_3$). Anal. Calcd. for $C_{29}H_{46}FN_3Si_2Zn$: C 60.34,, 8.03, N 7.28; found: C 60.90, H 8.22, N 7.14%.

2.2.12 | [L^7ZnN($SiMe_3$)$_2$] (7)

The same procedure as that of complex **1** was adopted. L^7H (0.55 g, 1.5 mmol) and zinc bis(trimethylsilyl)amide (0.58 g, 1.5 mmol) were used to afford light yellow crystals (325 mg, 37%). Mp: 197–199°C. ^{1}H NMR (400 MHz, 298 K, $CDCl_3$): δ 7.34 (s, 1H, Ar*H*), 7.12–6.95 (m, 4H, Ar*H*), 6.81 (t, ^3J = 6.8 Hz, 1H, Ar*H*), 6.72 (d, ^3J = 6.8 Hz, 1H, Ar*H*), 4.87 (s, 1H, γ-C*H*), 3.25 (sept, ^3J = 6.8 Hz, 1H, C*H*(CH_3)$_2$), 3.18 (sept, ^3J = 6.8 Hz, 1H, C*H*(CH_3)$_2$), 1.67 (s, 3H, CH_3), 1.61 (s, 3H, CH_3), 1.38 (d, ^3J = 6.8 Hz, 3H, CH(CH_3)$_2$), 1.33 (d, ^3J = 6.8 Hz, 3H, CH(CH_3)$_2$), 1.14 (d, ^3J = 6.8 Hz, 6H, CH(CH_3)$_2$), 0.09 (s, 18H, N(Si(CH_3)$_3$)$_2$). ^{13}C NMR (100 MHz, 298 K, $CDCl_3$): δ 170.3 (N*C*Me), 167.5 (N*C*Me), 150.1, 144.0, 142.1, 134.8, 130.0, 126.7, 126.5, 125.2, 124.4, 124.2 (all Ar-C), 96.6 (γ-*C*H), 28.8 (*C*H(CH_3)$_2$), 25.2 ($CH(CH_3)_2$), 24.8 ($CH(CH_3)_2$), 24.7 (NC-CH_3), 23.9 (NC-CH_3), 5.2 ($Si(CH_3)_3$). Anal. calcd. For $C_{29}H_{46}ClN_3Si_2Zn$: C 58.67, H 7.81, N 7.08; found: C 59.07, H 7.82, N 6.95%.

2.2.13 | [L^8ZnN($SiMe_3$)$_2$] (8)

The same procedure as that of complex **1** was adopted. L^8H (0.57 g, 1.5 mmol) and zinc bis(trimethylsilyl)amide (0.58 g, 1.5 mmol) were used to afford light yellow crystals (380 mg, 42%). Mp: 128–130°C. ^{1}H NMR (400 MHz, 298 K, $CDCl_3$): δ 7.22 (d, ^4J = 2.2 Hz, 1H, Ar*H*), 7.12–7.07 (m, 4H, Ar*H*), 6.96 (dd, ^3J = 8.3 Hz, ^4J = 2.2 Hz, 1H, Ar*H*), 6.75 (d, ^3J = 8.0 Hz, 1H, Ar*H*), 4.78 (s, 1H, γ-C*H*), 3.28 (sept, ^3J = 6.8 Hz, 1H, C*H*(CH_3)$_2$), 3.13 (sept, ^3J = 6.8 Hz, 1H, C*H*(CH_3)$_2$), 2.00 (s, 3H, CH_3), 1.61 (s, 3H, CH_3), 1.48 (s, 3H, CH_3), 1.38 (d, ^3J = 6.8 Hz, 3H, CH(CH_3)$_2$), 1.29 (d, ^3J = 6.8 Hz, 3H, CH(CH_3)$_2$), 1.13 (d, ^3J = 6.8 Hz, 3H, CH(CH_3)$_2$), 1.09 (d, ^3J = 6.8 Hz, 3H, CH(CH_3)$_2$), 0.20 (s, 9 H, N(Si(CH_3)$_3$)$_2$), − 0.15 (s, 9 H, N(Si(CH_3)$_3$)$_2$). ^{13}C NMR (100 MHz, 298 K, $CDCl_3$): δ 170.2 (N*C*Me), 168.1

(N*C*Me), 149.1, 144.0, 142.3, 141.9, 132.2, 132.0, 130.3, 126.6, 126.5, 125.6, 124.5 (Ar-*C*), 124.3 (all Ar-C), 95.9 (γ-*C*H), 28.5 ($CH(CH_3)_2$), 25.1 ($CH(CH_3)_2$), 24.6 ($CH(CH_3)_2$), 24.5 ($CH(CH_3)_2$), 24.4 ($CH(CH_3)_2$), 24.3 (NC-CH_3), 23.4 (NC-CH_3), 17.6 (Ar-CH_3), 5.5 ($Si(CH_3)_3$), 5.1 ($Si(CH_3)_3$). Anal. Calcd. for $C_{30}H_{48}ClN_3Si_2Zn$: C 59.29, H 7.96, N 6.91; found: C 58.76, H 7.77, N 6.62%.

2.3 | General polymerization procedures

2.3.1 | Ring-opening polymerization of *rac*-lactide

In a Braun Labstar glovebox (25°C), an initiator solution from a stock solution in THF or toluene was injected sequentially into a series of 10 ml Schlenk tubes loaded with *rac*-LA and suitable amounts of dry solvent. After specified time intervals, each Schlenk tube was taken out of the glovebox; an aliquot was withdrawn and quenched quickly with wet light petroleum ether, the reaction mixture was quenched at the same time by adding an excess amount of light petroleum ether and one drop of water. All of the volatiles in the aliquots were removed, and the residue was subjected to monomer conversion determination, which was monitored by integration of monomer versus polymer methine resonances in the ^{1}H NMR spectra ($CDCl_3$, 400 MHz, 298 K). The precipitates collected from the bulk mixture were dried in air, dissolved with CH_2Cl_2, and sequentially precipitated into methanol. The obtained polymer was further dried in a vacuum oven at 50°C for 16 h. In the cases where 2-propanol was used, the solution of initiator was injected into the solution of *rac*-LA and 2-propanol in toluene or THF. Otherwise, the procedures were the same.

2.3.2 | Ring-opening polymerization of ε-caprolactone

In a Braun Labstar glovebox (25°C), an initiator solution from a stock solution in toluene was injected sequentially into a series of 10 ml Schlenk tubes loaded with a solution of ε-caprolactone in toluene. After specified time intervals, each Schlenk tube was taken out of the glovebox; an aliquot was withdrawn and quenched quickly with wet light petroleum ether, the reaction mixture was quenched at the same time by adding an excess amount of light petroleum ether and one drop of water. All of the volatiles in the aliquots were removed (avoiding long time exposure to high vacuum), and the residue was subjected to monomer conversion determination via ^{1}H NMR spectroscopy ($CDCl_3$, 400 MHz, 298 K). The precipitates collected from the bulk mixture were dried in air, dissolved with CH_2Cl_2, and sequentially precipitated into methanol. The obtained polymer was further dried in a vacuum oven at 50°C for 16 h.

2.3.3 | Copolymerization of L-lactide and ε-caprolactone

In this study three different copolymerization methods were adopted:

Method A: copolymerization was started with ε-CL at specific temperature, after full conversion of ε-CL the polymerization was continued for desired time upon the sequential addition of *L*-LA. Aliquots were withdrawn for determination of the level of monomer conversions by ^{1}H NMR spectroscopy. The copolymerization mixture was quenched with wet petroleum ether and further treated with excess of methanol. The white precipitate was collected and dried in a vacuum oven at 60°C for 24 h. The copolymer was characterized by NMR spectroscopy, GPC and DSC analysis.

Method B: copolymerization was started with *L*-LA at desired temperature, after full conversion of *L*-LA the polymerization was continued for extended time at specific temperature upon the sequential addition of ε-CL. Otherwise, the procedures were the same.

Method C: copolymerization was started with equal amount of ε-CL and *L*-LA added at the same time at specific temperature. Otherwise, the procedures were the same.

2.4 | X-ray crystallography

Suitable crystals of complexes **4** and **6** for *X*-ray diffraction studies were obtained from a tetrahydrofuran-hexane mixture or a toluene-hexane mixture at −40°C or room temperature respectively. Diffraction data were collected on a Bruker AXSD 8 diffractometer. All data were collected at 20°C using the ω-scan techniques. All structures were solved by direct methods and refined using Fourier techniques. An absorption correction based on SADABS was applied.[24] All non-hydrogen atoms were refined by full-matrix least-square on F^2 using the SHELXTL program package.[25] Hydrogen atoms were located and refined by the geometry method. The cell refinement, data collection, and reduction were done by Bruker SAINT.[26] The structure solution and refinement were performed by SHELXS-97 and SHELX-97 respectively.[27] Molecular structures were generated using the ORTEP program.[28] For complex **4** $C_{32}H_{53}N_3Si_2Zn$, monoclinic, *P*21/n; a = 11.591(4) Å, b = 20.569(8) Å, c = 15.619(6) Å, $\alpha = \gamma = 90.00^o$, β = 103.074(5) ^{o}, Z = 4. For complex **6**, $C_{29}H_{46}FN_3Si_2Zn$, triclinic, *P*-1; a = 9.383(3) Å, b = 12.993(5) Å, c = 13.967(5) Å, α = 75.869(4)^o, β = 89.454(4)^o, γ = 82.405(4)^o, Z = 2.

3 | RESULTS AND DISCUSSION

3.1 | Synthesis of zinc complexes

For better understanding the ligand effects on the catalytic activity and selectivity of *β*-diketiminate zinc complexes toward the polymerization of cyclic esters, we designed several unsymmetrical *β*-diketimine proligands with various substitutes on the *ortho*-, *meta*- or *para*-position(s) of one *N*-phenyl group. As illustrated in Scheme 1, *β*-diketimine proligands **L^{1}H-L^{8}H** were synthesized according to a normal condensation pathway reported in the literature[11] and were characterized by ^{1}H, ^{13}C NMR and elemental analysis. Zinc silylamido complexes **1–8** bearing these unsymmetrical *β*-diketiminate ligand were prepared readily by treating $Zn[N(SiMe_3)_2]_2$ with the appropriate proligand at 80°C in toluene (Scheme 1) and isolated as pale yellow crystals in moderate yields of 53–62%.

With an aim of possessing structurally well-defined zinc alkoxide complexes, complexes **1–8** were further treated with equal amount of ^{i}PrOH respectively. Regardless the various substitution mode in the *β*-diketiminate ligand, all reactions gave no desired product of the type 'LZn(O^{i}Pr)', but the free ligand and some uncharacterizable zinc species, indicating the decomposition of these *β*-diketiminate zinc complexes upon exposing to protonic sources.

The ^{1}H NMR spectrum of zinc complex **1** indicates clearly the unsymmetrical coordination environment around the metal center. Both aromatic rings as well as the two backbone methyl groups exhibit different resonances. The chemical shift difference of *γ*-C*H* between complex **1** and the free ligand is about 0.029 ppm, smaller than those for earlier reported *β*-diketiminate zirconium complexes (0.50 ~ 0.80 ppm).[29] However, such a small chemical shift difference (0.029 ppm) between free ligand and complex excludes the chance of any interactions between the ligand backbone carbon atom and the zinc center. Williams's group reported similar results[9] for symmetric *β*-diketiminate zinc complexes, which also show ca. 0.03 ppm chemical shift difference. It is noteworthy that two different septets are displayed for the methine protons of two isopropyl groups in complex **1** as well as four separated doublets for the –CH(C*H*$_3$)$_2$ methyl groups due to the restricted rotation of the *N*-aryl groups. In addition, two $SiMe_3$ fragments of the complex also display two separated singlets, suggesting that the bulky isopropyl groups restrict the free rotation of both the aryl moiety and Zn–$N(SiMe_3)_2$ bond on the NMR time scale.

Complexes **2** and **8** show similar spectroscopic features as complex **1**; while complexes **3–7** show only one singlet for the silylamido group, which indicates the free rotation of Zn–$N(SiMe_3)_2$ bond. The methine protons of isopropyl groups in these complexes show two or three doublets with different chemical shifts. It might be due to the less steric bulkiness of the other *N*-aryl group, which releases the steric hindrance between the *N*-2,6-isopropylphenyl and the silyamido group and leads to partial or free rotation of *N*-aryl bond.

The molecular structures of complexes **4** and **6** were studied by X-*ray* diffraction determination. As shown in Figure 1, complex **4** possesses a monomeric structure in the solid state, where the Zn center is tri-coordinated by the *β*-diketiminate ligand and one silylamido group. The very close bond lengths of Zn1–*N* = 1.948(3) Å and Zn1–N2 = 1.950(3) Å, as well as C11–N1 = 1.329(4) Å and C13–N1 = 1.343(4) Å, indicate significant delocalization in the related bonds.[30] The two aryl rings have similar orientations toward the ligand backbone, with the dihedral angle of 118.3(3)° formed by the 2,6-diisopropylphenyl ring and that of (120.0(3)°) by

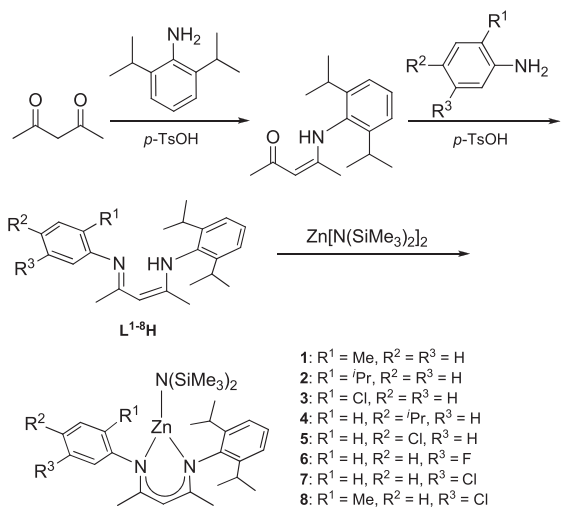

SCHEME 1 Synthesis of complexes **1–8**

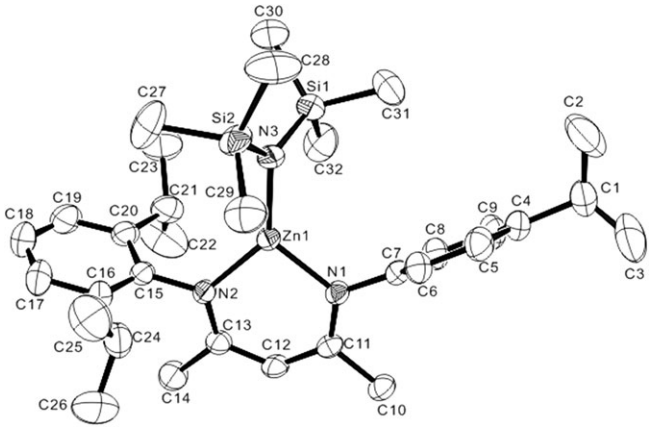

FIGURE 1 ORTEP view of the molecular structure of complex **4** (hydrogen atoms omitted for clarity). Selected bond lengths (Å) and angles (°): Zn1-N1 1.948(3), Zn1-N2 1.950(3), Zn1-N3 1.869(3), Si1-N3 1.705(3), Si2-N3 1.698(3), N1-Zn1-N2 99.35(12), N1-Zn1-N3 126.89(13), N2-Zn1-N3 133.74(13)

the 4-isopropylphenyl ring. The zinc metal center is deviating 0.13 Å from the N1–C11–C12–C13–N2 ligand backbone plane, which is slightly smaller than the corresponding angle of the other unsymmetric zinc complexes reported in literature (0.20 Å),[10] indicating that in complex **4** the zinc center is nearly coplanar with the ligand backbone. This could be further confirmed by a dihedral angle of 5.92 ° formed by Zn1–N1–N2 and N1–C11–C12–C13–N2.

Similar to complex **4**, complex **6** also possesses three-coordinated plane triangle geometry (Figure 2). The bond lengths of Zn1–N1 = 1.945(3) Å and Zn1–N2 = 1.953(2) Å are in the normal range reported in literature.[30] The negligible difference between C1–N1 = 1.340(4) Å and C3–N3 = 1.333(4) Å of the ligand backbone also indicates significant delocalization of these bonds. The zinc center is deviating 0.196 Å from N1– C1–C2–C3–N2 ligand backbone plane, which is slightly larger than that in complex **4**. Besides, the long distance of 5.616 Å between the F atom and zinc center further excludes any coordination interaction between the zinc center and F atom.

3.1.1 | Ring-opening polymerization of *rac*-lactide

These *β*-diketiminate zinc silylamido complexes were investigated as initiators for the ring-opening polymerization of *rac*-lactide at room temperature both in toluene and THF, and the related polymerization results are summarized in Table 1. All of these complexes could efficiently initiate the polymerization of *rac*-lactide with or without the addition of 2-propanol, affording high molecular weight PLAs with narrow to moderate distributions (M_w/M_n = 1.02 ~ 1.68).

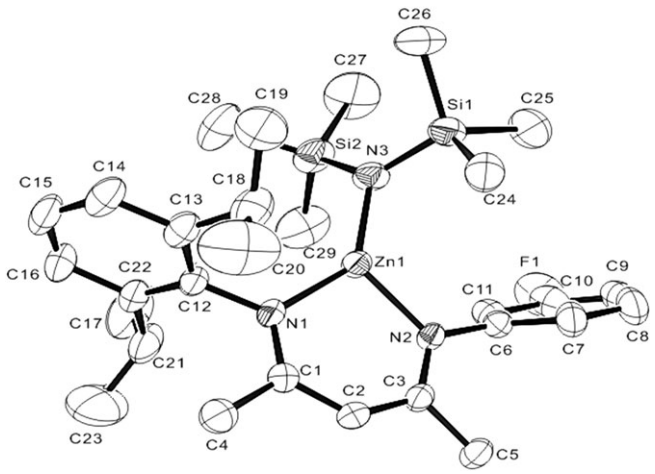

FIGURE 2 ORTEP view of the molecular structure of complex **6** (hydrogen atoms omitted for clarity). Selected bond lengths (Å) and angles (°): Zn1-N1 1.945(3), Zn1-N2 1.953(2), Zn1-N3 1.873(3), Si1-N3 1.714(3), Si2-N3 1.701(3), N1-Zn1-N2 99.16(10), N1-Zn1-N3 134.74(12), N2-Zn1-N3 126.08(12)

As shown in Table 1, with one *N*-aryl group being *N*-2,6-diisopropylphenyl, the substitution mode of the other *N*-aryl group of the *β*-diketiminate ligand has dramatic influence on the catalytic activity of these zinc silylamido complexes. In general, the introduction of a steric bulkier group on the *ortho*-position of the phenyl ring would lead to a decrease of the activity. For instance, when complex **1** (*o*-methyl) was adopted, a monomer conversion up to 94% could be achieved within 25 min in THF at room temperature (entry 1, TOF = 1128 h^{-1}, Table 1); a slightly lower monomer conversion of 91% was obtained by complex **2** (*o*-isopropyl) (entry 5, TOF = 1056 h^{-1}). However, a higher monomer conversion of 94% was achieved within 20 min by complex **4** (*p*-isopropyl) under otherwise the same reaction conditions (entry 13, TOF = 1410 h^{-1}). This might be attributed to that the steric bulky group at the *ortho*-position of the phenyl ring hinders the coordination/insertion of the lactide monomer to some extent. Similar phenomenon was reported by our group for the binapthyl-based iminophenolate magnesium complexes.[6g] However, Lin et al. reported[31] different steric effects for the tridentate *β*-diketiminate magnesium alkoxide complexes $[LMg(\mu\text{-OBn})]_2$, where the magnesium complex with the most steric hindered *tert*-butyl group displayed significantly higher activity than the 1,5-dimethyl substituted analogue. It is therefore conceivable that the introduction of two *N*-aryl rings to the ligand framework brings considerable steric hindrance to these complexes and an *ortho*-substituent of less steric bulkiness may be more favorable.

Both having a *para*-substituent on one of the phenyl rings, complex **4** with a *para*-isopropyl group showed slightly higher activity than complex **5** with a *para*-chloro group (entries 13 *vs*. 17). Meanwhile, complex **1** with an *ortho*-methyl group also showed slightly higher activity than *ortho*-Cl substituted complex **3** (entries 1 *vs*. 9). Therefore, the introduction of an electron withdrawing group at the *para*- or *ortho*-position of the phenyl ring seems to lead to a decrease of the catalytic activity. Similar effects were previously reported for magnesium complexes bearing *β*-ketiminate,[31] NNO tridentate iminophenolate,[32] and biphenyl-based tridentate iminophenolate ligands,[33] as well as for aluminum complexes reported by our group [20] and Tolman's group.[34] The authors figured that the introduction of electron-withdrawing groups causes the metal center to be more acidic, resulting in a stronger M − OR bond during polymerization, which retards the insertion of monomer.

Nevertheless, the effect of halogen substitution on activity is considerably complicated in this work. From a comparison of the catalytic activities of complexes **3**, **5** and **7**, an activity trend of **3** (*o*-Cl) < **7** (*m*-Cl) < **5** (*p*-Cl) could be observed (entries 9, 17 and 25), which is in contrast to those commonly reported in literature.[35] Furthermore, complexes **6** (*m*-F) and **7** (*m*-Cl) displayed the same activity. All these

TABLE 1 Ring-opening polymerization of *rac*-lactide initiated by zinc complexes **1** ~ **8** [a]

Entry	Cat.	$[LA]_0/[Zn]_0/[^iPrOH]_0$	Solv.	Time (min)	Conv.[b] (%)	TOF[c] (h^{-1})	$M_{n,calcd}$[d] ($\times 10^4$)	M_n [e] ($\times 10^4$)	M_w/M_n [e]	P_r[f]
1	**1**	500:1:0	THF	25	94	1128	6.77	21.5	1.12	0.82
2		500:1:1	THF	6	82	4100	5.92	7.42	1.05	0.81
3		500:1:0	Tol.	90	91	303	6.56	11.4	1.46	0.72
4		500:1:1	Tol.	25	88	1056	6.35	6.01	1.07	0.72
5	**2**	500:1:0	THF	25	91	1092	6.56	6.55	1.50	0.83
6		500:1:1	THF	8	95	3563	6.85	5.36	1.05	0.81
7		500:1:0	Tol.	90	80	267	5.77	13.5	1.44	0.74
8		500:1:1	Tol.	25	93	1104	6.71	5.21	1.12	0.73
9	**3**	500:1:0	THF	25	88	1056	6.34	10.1	1.18	0.79
10		500:1:1	THF	8	96	3600	6.92	6.04	1.06	0.80
11		500:1:0	Tol.	90	93	310	6.70	15.5	1.39	0.70
12		500:1:1	Tol.	20	95	1425	6.85	6.04	1.06	0.71
13	**4**	500:1:0	THF	20	94	1410	7.06	7.45	1.55	0.82
14		500:1:1	THF	6	96	4800	6.92	6.55	1.50	0.80
15		500:1:0	Tol.	60	86	430	6.20	24.8	1.27	0.70
16		500:1:1	Tol.	20	80	1200	6.20	5.83	1.06	0.71
17	**5**	500:1:0	THF	20	92	1380	6.63	8.02	1.39	0.81
18		500:1:1	THF	8	95	3563	6.85	5.38	1.10	0.80
19		500:1:0	Tol.	60	93	465	6.70	17.8	1.28	0.69
20		500:1:1	Tol.	20	84	1260	6.06	5.84	1.06	0.70
21	**6**	500:1:0	THF	25	93	1116	6.70	8.55	1.68	0.82
22		500:1:1	THF	6	94	4700	6.78	6.79	1.03	0.82
23		500:1:0	Tol.	90	86	287	6.20	26.3	1.53	0.64
24		500:1:1	Tol.	20	89	1335	6.42	6.02	1.06	0.64
25	**7**	500:1:0	THF	25	93	1116	6.70	15.0	1.18	0.80
26		500:1:1	THF	6	92	4600	6.64	6.85	1.06	0.80
27		500:1:0	Tol.	90	94	313	6.77	21.7	1.23	0.48
28		500:1:1	Tol.	20	95	1425	6.85	6.74	1.02	0.48
29	**8**	500:1:0	THF	25	79	948	5.69	28.1	1.15	0.83
30		500:1:1	THF	8	95	3563	5.70	4.43	1.10	0.82
31		500:1:0	Tol.	120	91	228	6.56	26.5	1.20	0.81
32		500:1:1	Tol.	20	92	1380	6.64	7.07	1.03	0.84

[a]$[rac\text{-LA}]_0 = 2.0$ M, 25 °C;

[b]Determined by ^{1}H NMR spectroscopy;

[c]Moles of LA consumed per mole of zinc per hour,

[d]$M_{n,calcd} = ([rac\text{-LA}]_0/[Zn]_0) \times 144.13 \times$ Conv.%

[e]Determined by GPC;

[f]P_r is the probability of forming a new *r*-dyad, determined by homonuclear decoupled ^{1}H NMR spectroscopy.

may indicate that the electronic effect is not obvious for this series of complexes. Complex **8** (2-Me-5-Cl) combines two kinds of effects, with an electron-withdrawing Cl group on the *meta*-position and a methyl group on the *ortho*-position of the phenyl ring, and is therefore least active, only achieving a monomer conversion of 79% within 25 min in THF.

As shown in Table 1, the polymerization medium also plays an important role in influencing the activity. All complexes showed higher catalytic activity in THF than in toluene. Taking complex **1** as an example, a monomer conversion of 94% could be achieved within 25 min in THF, whereas a conversion of 91% could only be achieved with extended polymerization time to 90 min in toluene (entries 1 and 3). Upon the addition of isopropanol, the activities of zinc silylamido complexes **1** ~ **8** increased significantly, high monomer conversions up to 95% could be

reached just within 20 ~ 25 min in toluene. When the polymerization was carried in THF, the reaction time could be decrease to 6 ~ 8 min although with a high molar ratio of $[LA]_0/[Zn]_0 = 500$.

To acquire some information on the ROP of *rac*-lactide initiated by the *in situ* generated zinc isopropoxide, an NMR-scale polymerization was conducted with $[rac\text{-}LA]_0$: $[\mathbf{1}]_0$: $[^i PrOH]_0 = 20$: 1: 1. The polymerization started instantaneously upon mixing and active oligomer could be identified (see Figure S21). The new resonances at 4.90 ppm (br) and 0.90 ppm (br) are assignable to an isopropoxyl terminal group. The singlet at 0.09 ppm indicates the quantitative formation of free $HN(SiMe_3)_2$. At the same time, no signals belonging to the free ligand could be detected in the NMR spectrum. Moreover, the ^1H NMR spectrum of the purified oligomer sample shows clearly the existence of both the hydroxyl and the isopropyl ester terminal groups (see Figure S22). All these facts suggest the initial generation of zinc isopropoxide species '[L^1ZnO^iPr]' from the reaction of zinc silylamido complex and isopropanol, which further initiate the polymerization of *rac*-LA via a coordination-insertion mechanism and produce linear PLAs with isopropyl ester and hydroxyl terminals.

Microstructure analyses of PLAs were achieved through inspecting the methine region of homonuclear decoupled ^1H NMR spectra of the resulting polymers. This series of zinc silylamido complexes demonstrate low to moderate stereoselectivity in toluene ($P_r = 0.48$ ~ 0.84) and relatively higher stereoselectivity in THF ($P_r = 0.79$ ~ 0.83). A similar trend of solvent effect on the stereoselectivity was reported by Chisholm and co-workers for β-diiminate magnesium complexes L'Mg^{n}Bu(THF), which showed higher heteroselectivity in THF than in a toluene–dichloromethane mixture.[36]

Although zinc complexes **1**–**8** show similar heteroselectivities in THF, the nature of ligand substituents does have certain impact on the stereoselectivity of these complexes in toluene. Among them, complex **8** (2-methyl-5-Cl) displays the highest heteroselectivity of $P_r = 0.81$ in the absence of isopropanol (entry 31). The heteroselectivity of complex **2** (*o*-isopropyl) decreases to 0.74; by using the less steric bulky complex **1** (*o*-methyl) as the initiator, the heteroselectivity further decreases to 0.72 (entry 3). Lower heteroselectivities around 0.70 (entries 15 and 19) are observed for complexes **4** and **5** with *para*-substituted phenyl ring. It is noteworthy that, complexes **6** and **7** which contain an electron-withdrawing group on the *meta*-position of the phenyl ring exhibit significantly lower heteroselectivity in the whole series (**6**: 0.64, entry 23; **7**: 0.48, entry 27). All these however are consistent with the literature reports that lower steric demand at the *ortho* position is generally found to reduce the control in stereoselectivity to heterotactic PLAs.[7, 8r]

3.1.2 | Ring-opening polymerization of ε-caprolactone

Before conducting ε-CL/LA copolymerization, homopolymerization of ε-caprolactone at room temperature initiated by these β-diketiminate zinc silylamido complexes was carried out.

As shown in Table 2, the substituents, particularly the one at the *ortho*-position of the phenyl ring, play an important role in determining the polymerization activity. For instance, by using complex **1** (*o*-methyl) as the initiator, a monomer conversion up to 96% could be achieved within 30 min (entry 1, Table 2). Complex **2** with a sterically bulkier *ortho*-isopropyl group showed a lower activity, giving a monomer conversion of 89% within 40 min (entry 2). However, complex **4** with a *para*-substituted *N*-phenyl ring was found to be less active than complexes **1** and **2**, reaching 85% monomer conversion within 50 min at room temperature (entry 4). It was previously reported[6b] that the presence of bulky groups in the coordination sphere of the central metal tends to block the coordination/insertion of incoming monomer and hence is disadvantageous to the catalytic activity. However, in this system, an appropriate steric bulky substituent on the phenyl ring is favorable for the increase of the polymerization activity.

Likely due to the introduction of an electron-withdrawing group at the *meta*-position of the phenyl ring, complexes **6** and **7** showed higher activities than complexes **3** and **5** with *ortho*- or *para*-substituted *N*-phenyl ring. The increase of activity of complex **8** further confirmed the combined consequence of the above mentioned steric and electronic effects.

Generally, the ROPs of ε-caprolactone initiated by these zinc silylamido complexes are not well-controlled, giving moderately distributed polymers (M_w/M_n = 1.31–1.71),

TABLE 2 Ring-opening polymerization of ε-CL initiated by zinc complexes [a]

Entry	Cat.	Time (min)	Conv.[b] (%)	$M_{n,calcd}$[c] ($\times 10^4$)	M_n[d] ($\times 10^4$)	M_w/M_n[d]
1	**1**	30	96	3.28	5.25	1.55
2	**2**	40	89	2.96	4.50	1.71
3	**3**	40	91	3.11	8.07	1.44
4	**4**	50	85	3.29	11.8	1.45
5	**5**	50	95	3.25	11.9	1.42
6	**6**	30	99	3.39	6.93	1.67
7	**7**	30	97	3.32	15.0	1.31
8	**8**	8	93	3.18	25.8	1.39

[a]$[\varepsilon\text{-CL}]_0 = 1.5$ M, $[\varepsilon\text{-CL}]_0/[Zn]_0 = 300{:}1$, at 25°C, in toluene;

[b]Determined by ^1H NMR spectroscopy;

[c]$M_{n,calcd} = ([\varepsilon\text{-CL}]_0/[Zn]_0) \times 114.14 \times$ Conv.%;

[d]Determined by GPC.

which is normally attributed to the less nucleophilic nature of the silylamido group and therefore the relatively slow initiation during the polymerization.

3.1.3 | Copolymerization of L-lactide and ε-caprolactone

According to the previous literature report,[37] diblock copolymers of lactide and ε-caprolactone could be produced by the sequential polymerization of lactide after the full conversion of ε-caprolactone. However, it would be difficult if the order is reversed or a one-pot polymerization strategy is adopted. Herein, we chose complex **6**, which showed moderate activity for *rac*-lactide polymerization and meanwhile relatively high activity for ε-caprolactone polymerization, to explore the ability of this series of β-diketiminate zinc complexes for the copolymerization of *L*-lactide and ε-caprolactone. The copolymerization runs were carried out via three different feeding methods in toluene; the results are summarized in Table 3. T3

Synthesis of PCL-*b*-PLLA

Initially, the copolymerization was carried out *via* a sequential addition of *L*-LA after the full conversion of ε-CL (method A). Equal amount of *L*-LA monomer was added to the flask after the full conversion of ε-CL (99%) in 30 min at r.t. and then the reaction was kept for additional 8 h at the same temperature. Only 18% of lactide was converted according to the ^{1}H NMR spectrum of the resultant mixture (entry 1, Table 3). By either raising the reaction temperature of the second stage for *L*-LA polymerization or carrying the whole copolymerization in the presence of alcohol, significant acceleration of the polymerization process could be observed. *L*-LA conversion of 59% could be achieved at 60°C in 2 h at the second stage (entry 2). In the presence of 1 equiv. of isopropanol, *L*-LA conversion of 67% was reached within 6 h at r.t. (entry 3). In this case, the molecular weight of obtained polymer sample is quite close to the calculated one and the molecular weight distribution is very narrow (PDI = 1.04), indicating a well-controlled polymerization process.

To explore the microstructure of resultant copolymer, ^{1}H and ^{13}C NMR spectroscopy as well as DSC analysis were carried out (Figure 3, S25 and S27). The small resonance appearing at 4.13 ppm in the ^{1}H NMR spectrum (Figure 3). is assignable to the CL-LA linkages of the copolymer, which indicates the presence of block structures. In the ^{13}C NMR spectrum, two carbonyl resonances at 169.8 ppm and 173.8 ppm are displayed (Figure S25), corresponding to the long blocks of -LLLLLL- ('L' represents half of a lactide unit) and -CapCapCap- units respectively.[12–14] Besides, no other signals including the one at 170.8 ppm attributable to –CapLCap- triad arising from transesterifications[20] could be observed. The relatively narrow molecular weight distribution in mono-model together with these spectroscopic features gives evidence to the formation of a block copolymer. From its DSC curve (Figure S27), two melting peaks at 51.19°C and 165.79°C are shown, which correspond to T_m of long PCL and PLA blocks respectively. These results match well with the literature reports,[38,39] and further confirm the formation of diblock copolymer PCL-*b*-PLLA.

Synthesis of PLLA-*b*-PCL

To verify the possibility of 'PLA-block-first route', sequential ROP of *L*-LA and ε-caprolactone by complex **6** was assessed in toluene (method B). From the data shown in Table 3, it was found that after the full conversion of *L*-LA in 1 h at r.t., the polymerization continued when ε-CL was added sequentially, although the polymerization became very retard – a ε-CL conversion of 50% was only achieved after extended 12 h (entry 4). With the presence of 1 equiv. of isopropanol, both of the two polymerization stages were accelerated, a similar ε-CL conversion of 56% could be achieved after extended 6 h, meanwhile resulting in polymers with a very narrow PDI (M_w/M_n = 1.07, entry 5). Similar to the previous case, characterization of the polymer sample with NMR spectroscopy and DSC analysis indicates again the formation of a diblock copolymer (Figures S23, S26 and S28), which shows two melting peaks (T_m) at 53.81°C for PCL block and 166.08°C for PLLA block.

It is noteworthy that, normally it is difficult to polymerize ε-CL with living PLA* blocks because of the resting state of the active metal center formed during the ROP of LA which involves the chelation of the growing polymer chain *via* formation of a five-membered ring. It appears that this chelation effectively shuts down the sequential ROP of ε-CL monomer.[39] Therefore, there are very limited literature reports about aluminum complexes that copolymerize ε-CL after the initial polymerization of LA to achieve diblock copolymers.[37,40] This is the first successful attempt that diblock copolymerizations of ε-CL and *L*-LA are realized by zinc silylamido complex via two different feeding strategies to gain desired PCL-*b*-PLLA and PLLA-*b*-PCL copolymers without clear transesterification side reaction.

Synthesis of PLLA-*b*-PCL copolymer via one-pot polymerization method

Last but not least, copolymerization was carried out by one-pot polymerization method (method C) *via* the addition of two monomers at the same time at ambient temperature. The results showed that after the full conversion of *L*-LA in 3 h only 2% of ε-CL monomer was converted (entry 6, Table 3); the ε-CL conversion increased to 15% after extending the reaction time to 8 h at r.t. (entry 7). To further improve the monomer conversion of ε-CL, the reaction

TABLE 3 Copolymerization of *L*-LA and *ε*-CL initiated by zinc complex **6**[a]

	Stage 1						Stage2								
Entry	Meth.	[CL] /[Zn]	[LA] /[Zn]	t_1 (h)	Conv. of CL[b] (%)	Conv. of LA[b] (%)	[CL] /[Zn]	[LA] /[Zn]	t_2 (h)	Conv. of CL [b] (%)	Conv. of LA [b] (%)	LA/CL in co-polym.[c] (%)	$M_{n,calcd}$ [d] ($\times 10^4$)	M_n[e] ($\times 10^4$)	M_w/M_n[e]
1	(A)	300	---	0.5	99	---	---	300	8	100	18	15/85	4.20	4.56	1.46
2[f]	(A)	300	---	0.5	99	---	---	300	2	100	59	37/63	5.58	18.2	1.41
3[h]	(A)	300	---	0.25	100	---	---	300	6	100	67	40/60	6.32	6.17	1.04
4	(B)	---	300	1	---	100	300	---	12	50	100	67/33	6.03	17.8	1.43
5[h]	(B)	---	300	0.25	---	100	300	---	6	56	100	64/36	5.85	5.35	1.07
6	(C)	300	300	3	2	100	---	---	---	---	---	98/2	4.39	5.28	1.49
7	(C)	300	300	8	15	100	---	---	---	---	---	87/13	4.83	2.60	1.37
8[g]	(C)	300	300	0.25	0	63	---	---	---	---	---	63/0	2.72	5.11	1.36
9[g]	(C)	300	300	0.5	4.3	96	---	---	---	---	---	96/4	4.30	5.94	1.38
10[g]	(C)	300	300	8	60	100	---	---	---	---	---	63/37	6.38	8.79	1.63
11[g]	(C)	300	300	22	80	100	---	---	---	---	---	56/44	7.06	12.7	1.62
12[g, h]	(C)	300	300	4	50	100						67/33	6.04	5.97	1.39

[a]All polymerizations were carried out in toluene at r.t. except for runs 2 and 6–9; $[\varepsilon\text{-CL}]_0 = [L\text{-LA}]_0 = 1.5$ M;

[b]Determined by ^{1}H NMR spectroscopy;

[c]LA/CL mole ratio in the copolymer;

[d]$M_{n,calcd} = ([CL]_0/[Zn]_0) \times 114.14 \times \text{Conv.}\% + ([LA]_0/[Zn]_0) \times 144.13 \times \text{Conv.}\%$;

[e]Determined by gel permeation chromatography in tetrahydrofuran, calibrated with polystyrene standards;

[f]*L*-LA was polymerized at 60 °C after the full conversion of *ε*-CL at 25 °C;

[g]Polymerization was carried out at 60 °C;

[h]polymerizations were carried out in the presence of 1 equiv. of ^{i}PrOH.

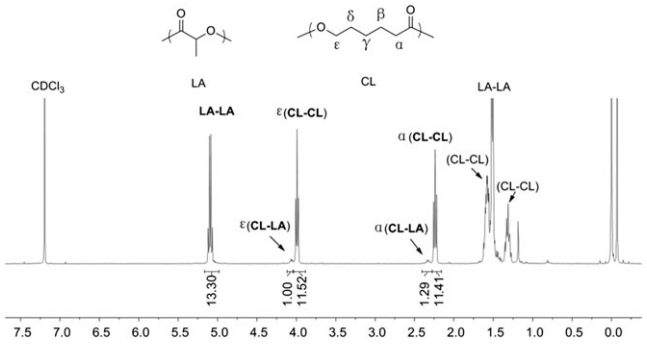

FIGURE 3 The ^{1}H NMR spectrum of (PCL-*b*-PLLA) obtained via method a ($CDCl_3$, 400 MHz; Table 3, entry 2)

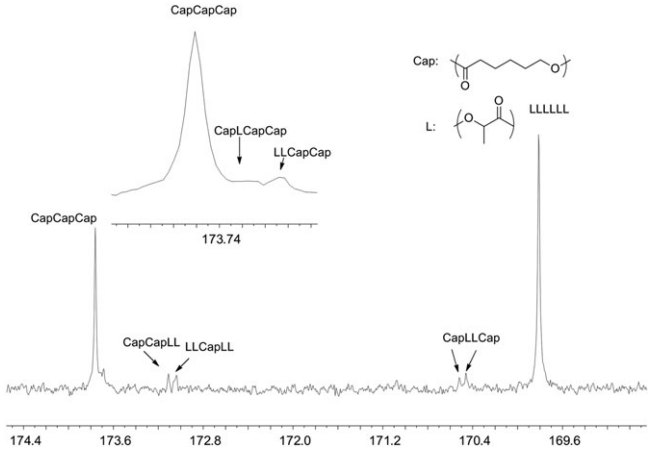

FIGURE 4 ^{13}C NMR spectrum of (PLLA-*b*-PCL) copolymer obtained via one-pot polymerization method ($CDCl_3$, 400 MHz; Table 3, entry 11)

temperature was increased to 60°C. After 0.5 h of polymerization, monomer conversions of 96% and 4.3% were achieved for *L*-LA and *ε*-CL respectively (entry 9); the *ε*-CL conversion increased slowly with the prolongation of polymerization time, which finally reached to 80% in 22 h (entry 11). The polymerization process could be drastically shortened to 4 h with the addition of isopropanol at 60°C (PLA: 100%; PCL = 50%). Furthermore, the narrow polydispersity of the resultant copolymer indicated that the copolymerization proceeded in a well-controlled manner (PDI = 1.39; entry 12). It is worthy of noting that, complex **6** shows higher activity for the homo-polymerizations of *rac*-LA and *ε*-CL at ambient temperature. However, higher reaction temperature and longer reaction time are required for copolymerization, just similar to those reported by Chisholm.[41]

From the ^{1}H NMR spectrum of typical copolymer sample (entry 11, Figure S24), it is found that the resonance at 4.13 ppm attributable to the CL-LA linkages of the polymer chain is more obvious than the previous cases, suggesting higher content of CL-LA linkages in the copolymer. Being consistent with this observation, in the ^{13}C NMR spectrum of this sample (Figure 4). besides the two dominant carbonyl signals at 169.8 ppm and 173.8 ppm assignable to -LLLLLL- and -CapCapCap- triads, small signals at around 173.1 ppm and 170.5 ppm are also observed in the carbonyl region, which belong to CapCapLL/LLCapLL and CapLLCap triads according to literature reports.[12–14,20] All these suggest the insertion of *ε*-CL monomer into *L*-LA dominant blocks and *vice versa*. Notably, there is no peak at 170.8 ppm arising from the CapLCap unit, excluding any transesterification reactions during the polymerization process. Furthermore, two small melting peaks at 43.44°C and 168.42°C attributable to PCL and PLA blocks are displayed in the DSC diagram of this sample (Figure S29),[37,38] In comparison with the diblock copolymers obtained via methods A and B, the PLA block of this copolymer sample shows a similar melting point indicating normally long –LLLLLLL- sequences, but the melting point of PCL block decreases obviously, which may suggest shorter lengths of …CapCapCapCapCap… sequences.

Although relatively broad molecular weight distribution is witnessed for the same sample from the GPC measurement (PDI = 1.62), it still shows monodisperse nature. Taking all the above-mentioned results into consideration, we suggest that, when adopting the one-pot strategy, this series of *β*-diketiminate zinc silylamido complexes could initiate *ε*-CL polymerization after achieving high *L*-lactide conversion to form a copolymer with essentially diblock nature; during this process, small amount of *ε*-CL monomer would insert into the PLA block occasionally, the rest of lactide monomer would also insert into the PCL block when *ε*-CL polymerization started after the consumption of most of *L*-LA monomer. Therefore, the copolymer obtained via method C contains more defects than those obtained via the other two methods.

In an attempt to characterize the end-groups of the copolymers, one-pot copolymerization of *L*-LA and *ε*-CL was carried out on a NMR scale in C_6D_6 at 60°C with or without the addition of isopropanol. The MALDI-TOF mass spectra of obtained copolymer samples indicate the incorporation of both monomers in the oligomer chain, although in both cases cyclic copolymers were detected dominantly, likely due to the overlong polymerization period inevitably leading to undesired transesterifications (Figures S30-S31).

4 | CONCLUSIONS

Monometallic *β*-diketiminate zinc silylamido complexes **1**–**8** have been synthesized and fully characterized. These zinc complexes show satisfied catalytic activities toward the ring-opening polymerization of *rac*-Lactide, producing heterotactic PLAs with high molecular weights and narrow to moderated molecular weight distributions (PDI = 1.02–1.68).

The structure of ligands as well as the polymerization medium exerts obvious impact on the catalytic performance of these complexes. Zinc complexes **1–8** also show good activities for the ROP of ε-caprolactone at ambient temperature, forming PCLs with moderate PDIs (PDI = 1.31–1.71). Most importantly, diblock copolymerization of *L*-lactide and ε-caprolactone could be realized by zinc complex **6** under various temperatures via three different feeding methods (sequential addition of two monomers in either order and one-pot reaction). The one-pot copolymerization strategy led to diblock copolymers with more random linkages along the polymer chain especially in the PCL block, as characterized by NMR spectroscopy and DSC analysis.

ACKNOWLEDGEMENTS

Financial supports from the National Natural Science Foundation of China (NNSFC, 21074032 and 21474028) and the Fundamental Research Funds for the Central Universities (WD1113011) are gratefully acknowledged. H. Ma also thanks the very kind donation of a Braun glove-box by AvH foundation.

REFERENCES

[1] a) J. Fernandez, A. Etxeberria, J.-R. Sarasua, *J. Appl. Polym. Sci.* **2015**, *132*, 42520; b) S. M. Guillaume, E. Kirillov, Y. Sarazin, J.-F. Carpentier, *Chem.–Eur. J.* **2015**, *21*, 7988; c) S. Dagorne, M. Normand, E. Kirillov, J.-F. Carpentier, *Coord. Chem. Rev.* **2013**, *257*, 1869; d) P. J. Dijkstra, H. Du, J. Feijen, *Polym. Chem.* **2011**, *2*, 520; e) J. C. Buffet, J. Okuda, *Polym. Chem.* **2011**, *2*, 2758; f) C. M. Thomas, *Chem. Soc. Rev.* **2010**, *39*, 165; g) A. K. Sutar, T. Maharana, S. Dutta, C.-T. Chen, C.-C. Lin, *Chem. Soc. Rev.* **2010**, *39*, 1724; h) M. J. Stanford, A. P. Dove, *Chem. Soc. Rev.* **2010**, *39*, 486; i) R. H. Platel, L. M. Hodgson, C. K. Williams, *Polym. Rev.* **2008**, *48*, 11; j) R. Hoogenboom, U. S. Schubert, *Chem. Soc. Rev.* **2006**, *35*, 622; k) O. Dechy-Cabaret, B. Martin-Vaca, D. Bourissou, *Chem. Rev.* **2004**, *104*, 6147.

[2] L. B. Calvo, M. G. Davidson, D. García-Vivó, *Inorg. Chem.* **2011**, *50*, 3589.

[3] W.-Y. Lu, M.-W. Hsiao, S. C. N. Hsu, W.-T. Peng, Y.-J. Chang, Y.-C. Tsou, T.-Y. Wu, Y.-C. Lai, Y. Chen, H.-Y. Chen, *Dalton Trans.* **2012**, *41*, 3659.

[4] S. C. Roşca, D. A. Roşca, V. Dorcet, C. M. Kozak, F. Kerton, J.-F. Carpentier, Y. Sarazin, *Dalton Trans.* **2013**, *42*, 9361.

[5] R. K. Dean, A. M. Reckling, H. Chen, L. N. Dawe, C. M. Schneider, C. M. Kozak, *Dalton Trans.* **2013**, *42*, 3504.

[6] a) A. Grala, J. Ejfler, L. B. Jerzykiewicz, P. Sobota, *Dalton Trans.* **2011**, *40*, 4042; b) L. Wang, H. Ma, *Macromolecules* **2010**, *43*, 6535; c) H.-Y. Chen, L. Mialon, K. A. Abboud, S. A. Miller, *Organometallics* **2012**, *31*, 5252; d) Y. Wang, W. Zhao, D. Liu, S. Li, X. Liu, D. Cui, X. Chen, *Organometallics* **2012**, *31*, 4182; e) J. P. Davin, J.-C. Buffet, T. P. Spaniol, J. Okuda, *Dalton Trans.* **2012**, *41*, 12612; f) B. Liu, T. Roisnel, J.-P. Guégan, J.-F. Carpentier, Y. Sarazin, *Chem.–Eur. J.* **2012**, *18*, 6289; g) M. Huang, C. Pan, H. Ma, *Dalton Trans.* **2015**, *44*, 12420.

[7] a) Y. Sarazin, B. Liu, T. Roisnel, L. Maron, J.-F. Carpentier, *J. Am. Chem. Soc.* **2011**, *133*, 9069; b) L. Wang, H. Ma, *Dalton Trans.* **2010**, *39*, 7897; c) S. Song, X. Zhang, H. Ma, Y. Yang, *Dalton Trans.* **2012**, *41*, 3266; d) H. Wang, H. Ma, *Chem. Commun.* **2013**, *49*, 8686; e) R. Olejník, M. Bílek, Z. Ruzickova, Z. Hostalek, J. Merna, A. Ruzicka, *J. Organomet. Chem.* **2015**, *794*, 237; f) O. S. Trofymchuk, C. G. Daniliuc, G. Kehr, G. Erker, R. S. Rojas, *RSC Adv.* **2015**, *5*, 21054; g) C. Fliedel, V. Rosa, F. M. Alves, A. M. Martins, T. Avilés, S. Dagorne, *Dalton Trans.* **2015**, *44*, 12376; h) Y. Sun, Y. Cui, J. Xiong, Z. Dai, N. Tang, J. Wu, *Dalton Trans.* **2015**, *44*, 16383; i) D. Jędrzkiewicz, J. Ejfler, N. Gulia, Ł. John, S. Szafert, *Dalton Trans.* **2015**, *44*, 13700; j) Q. Shi, J. Yang, X. Lü, *Inorg. Chem. Commun.* **2015**, *59*, 61; k) M. Chisholm, J. Huffman, K. Phomphrai, *J. Chem. Soc. Dalton Trans.* **2001**, 222; l) M. Chisholm, J. Gallucci, K. Phomphrai, *Inorg. Chem.* **2002**, *41*, 2785; m) H.-Y. Chen, B.-H. Huang, C.-C. Lin, *Macromolecules* **2005**, *38*, 5400; n) M. H. Chisholm, J. C. Gallucci, K. Phomphrai, *Inorg. Chem.* **2005**, *44*, 8004; o) C. N. Ayala, M. H. Chisholm, J. C. Gallucci, C. Krempner, *Dalton Trans.* **2009**, 9237; p) A. Kronast, M. Reiter, P. T. Altenbuchner, C. Jandl, A. Poethig, B. Rieger, *Organometallics* **2016**, *35*, 681.

[8] B. M. Chamberlain, M. Cheng, D. R. Moore, T. M. Ovitt, E. B. Lobkovsky, G. W. Coates, *J. Am. Chem. Soc.* **2001**, *123*, 3229.

[9] A. Dove, V. Gibson, E. Marshall, A. White, D. Williams, *Dalton Trans.* **2004**, *4*, 570.

[10] F. Drouin, P. Oguadinma, T. Whitehorne, R. Prudhomme, F. Schaper, *Organometallics* **2010**, *29*, 2139.

[11] S. Gong, H. Ma, *Dalton Trans.* **2008**, 3345.

[12] a) G. Li, M. Lamberti, D. Pappalardo, C. Pellecchia, *Macromolecules* **2012**, *45*, 8614; b) F. Qian, K. Liu, H. Ma, *Chin. J. Catal.* **2011**, *32*, 189; c) C. Kan, H. Ma, *RSC Adv.* **2016**, *6*, 47402.

[13] a) D. J. Darensbourg, O. Karroonnirum, *Macromolecules* **2010**, *43*, 8880; b) M. Honrado, A. Otero, J. Fernández-Baeza, L. F. Sánchez-Barba, A. Garcés, A. Lara-Sánchez, A. M. Rodríguez, *Organometallics* **2016**, *35*, 189.

[14] D. J. Gilmour, R. L. Webster, M. R. Perry, L. L. Schafer, *Dalton Trans.* **2015**, *44*, 12411.

[15] F. Bonnet, A. R. Cowley, P. Mountford, *Inorg. Chem.* **2005**, *44*, 9046.

[16] L. Fan, Y. Xiong, H. Xu, Z. Shen, *Eur. Polym. J.* **2005**, *41*, 1647.

[17] M. Lahcini, P. M. Castro, M. Kalmi, M. Leskala, T. Repo, *Organometallics* **2004**, *23*, 4547.

[18] J. L. Wang, C. M. Dong, *Macromol. Chem. Phys.* **2006**, *207*, 554.

[19] N. Nomura, A. Akita, R. Ishii, M. Mizuno, *J. Am. Chem. Soc.* **2010**, *132*, 1750.

[20] Y. Wang, H. Ma, *Chem. Commun.* **2012**, *48*, 6729.

[21] A. Pilone, N. De Mai, K. Press, V. Venditto, D. Pappalardo, M. Mazzeo, C. Pellecchia, M. Kol, M. Lamberti, *Dalton Trans.* **2015**, *44*, 2157.

[22] M. Honrado, A. Otero, J. Fernández-Baeza, L. F. Sánchez-Barba, A. Garcés, A. Gustín Lara-Sánchez, A. M. Rodríguez, *Organometallics* **2016**, *35*, 189.

[23] H. Bürger, W. Sawodny, U. Wannagat, *J. Organomet. Chem.* **1965**, *3*, 113.

[24] SADABS, Bruker Nonius area detector scaling and absorption correction-V 2.05, Bruker AXS Inc., Madison, WI, 1996.

[25] G. M. Sheldrick, SHELXTL 5.10 for Windows NT, Structure Determination Software Programs, Bruker Analytical X-ray Systems, Inc., Madison, WI, **1997**.

[26] SAINT, version 6.02, Bruker AXS Inc., Madison, WI, 1999; 53711–5373.

[27] G. M. Sheldrick, *SHELXS-97, Program for the Solution of Crystal Structures*, University of Góttingen, Germany **1990**.

[28] L. J. Farrugia, *J. Appl. Crystallogr.* **1997**, *30*, 565. ORTEP-III for Windows, Version 2.0, University of Glasgow, **2008**.

[29] S. Gong, H. Ma, J. Huang, *Dalton Trans.* **2009**, 8237.

[30] M. Cheng, D. Moore, J. Reczk, B. Chamberlain, E. Lobkovsky, G. Coates, *J. Am. Chem. Soc.* **2001**, *123*, 8738.

[31] H.-Y. Tang, H.-Y. Chen, J.-H. Huang, C.-C. Lin, *Macromolecules* **2007**, *40*, 8855.

[32] W.-C. Hung, C. -nLin, *Inorg. Chem.* **2009**, *48*, 728.

[33] W. Yi, H. Ma, *Dalton Trans.* **2014**, *43*, 5200.

[34] L. Alcazar-Roman, B. J. O'Keefe, M. Hillmyer, W. Tolman, *Dalton Trans.* **2003**, 3082.

[35] a) S. Gong, H. Ma, *Dalton Trans.* **2008**, 3345; b) F. Qian, K. Liu, H. Ma, *Dalton Trans.* **2010**, *39*, 8071; c) N. Iwasa, S. Katao, J. Liu, M. Fujiki, Y. Furukawa, K. Nomura, *Organometallics* **2009**, *28*, 2179.

[36] M. Chisholm, K. Choojun, J. Gallucci, P. Wambua, *Chem. Sci.* **2012**, *3*, 3445.

[37] D. Pappalardo, L. Annunziata, C. Pellecchia, *Macromolecules* **2009**, *42*, 6056.

[38] S. Wang, L. Lu, J. Gruetzmacher, B. Currier, M. Yaszemski, *Macromolecules* **2005**, *38*, 7358.

[39] J. Sarasua, N. Rodríguez, A. Arraiza, E. Meaurio, *Macromolecules* **2005**, *38*, 8362.

[40] Y. Liu, W. S. Dong, J.-Y. Liu, Y.-S. Li, *Dalton Trans.* **2014**, *43*, 2244.

[41] V. Balasanthiran, M. H. Chisholm, K. Choojun, C. B. Durr, *Dalton Trans.* **2014**, *43*, 2781.

SUPPORTING INFORMATION

Additional Supporting Information may be found online in the supporting information tab for this article.

How to cite this article: Keram M, Ma H. Ring-opening polymerization of lactide, ε-caprolactone and their copolymerization catalyzed by β-diketiminate zinc complexes. *Appl Organometal Chem.* 2017;e3893. https://doi.org/10.1002/aoc.3893